

Purdue University Purdue e-Pubs

Birck and NCN Publications

Birck Nanotechnology Center

10-2009

Gate-induced g-factor control and dimensional transition for donors in multivalley semiconductors

Rajib Rahman

Purdue University - Main Campus

Seung H. Park

Purdue University - Main Campus

Timothy B. Boykin

University of Alabama - Huntsville

Gerhard Klimeck

Network for Computational Nanotechnology, Purdue University, gekco@purdue.edu

Sven Rogge

Delft Univ Technol

See next page for additional authors

Follow this and additional works at: <http://docs.lib.purdue.edu/nanopub>



Part of the [Nanoscience and Nanotechnology Commons](#)

Rahman, Rajib; Park, Seung H.; Boykin, Timothy B.; Klimeck, Gerhard; Rogge, Sven; and Hollenberg, Lloyd CL, "Gate-induced g-factor control and dimensional transition for donors in multivalley semiconductors" (2009). *Birck and NCN Publications*. Paper 487. <http://docs.lib.purdue.edu/nanopub/487>

This document has been made available through Purdue e-Pubs, a service of the Purdue University Libraries. Please contact epubs@purdue.edu for additional information.

Authors

Rajib Rahman, Seung H. Park, Timothy B. Boykin, Gerhard Klimeck, Sven Rogge, and Lloyd CL Hollenberg

Gate-induced g -factor control and dimensional transition for donors in multivalley semiconductorsRajib Rahman,^{1,*} Seung H. Park,¹ Timothy B. Boykin,² Gerhard Klimeck,^{1,3} Sven Rogge,⁴ and Lloyd C. L. Hollenberg^{5,†}¹*Network for Computational Nanotechnology, Purdue University, West Lafayette, Indiana 47907, USA*²*Department of Electrical Engineering, University of Alabama, Huntsville, Alabama 35899, USA*³*Jet Propulsion Laboratory, California Institute of Technology, Pasadena, California 91109, USA*⁴*Kavli Institute of Nanoscience, Delft University of Technology, Lorentzweg 1, 2628 CJ Delft, The Netherlands*⁵*Center for Quantum Computer Technology, School of Physics, University of Melbourne, Victoria 3010, Australia*

(Received 17 August 2009; published 1 October 2009)

The dependence of the g factors of semiconductor donors on applied electric and magnetic fields is of immense importance in spin-based quantum computation and in semiconductor spintronics. The donor g -factor Stark shift is sensitive to the orientation of the electric and magnetic fields and is strongly influenced by the band-structure and spin-orbit interactions of the host. Using a multimillion atom tight-binding framework, the spin-orbit Stark parameters are computed for donors in multivalley semiconductors, silicon, and germanium. Comparison with limited experimental data shows good agreement for a donor in silicon. Results for gate-induced transition from three-dimensional to two-dimensional wave-function confinement show that the corresponding g -factor shift in Si is experimentally observable, and at modest B field, $O(1\text{ T})$ can exceed the Stark shift of the hyperfine interaction.

DOI: [10.1103/PhysRevB.80.155301](https://doi.org/10.1103/PhysRevB.80.155301)

PACS number(s): 71.55.Cn, 03.67.Lx, 71.70.Ej, 85.35.Gv

I. INTRODUCTION

Understanding the behavior of single donor-electron bound states under mesoscopic electric and magnetic fields is a fundamental issue critical to current miniaturization of semiconductor devices¹ and to the development of new quantum technologies.^{2–4} It is only very recently that convergence between experiment and theory has occurred for the electric gate control of the orbital states¹ and electron-nuclear hyperfine (HF) interaction^{5,6} for a donor in silicon. However, the Stark shift of the donor spin-orbit (SO) interaction, which is central to understanding the precise spin properties in combined electric and magnetic fields, is just beginning to be understood.⁷ We report an atomistic treatment of the donor spin-orbit interaction in multivalley semiconductors in gated environments and show nontrivial agreement with experiment where available. We calculate the donor g -factor shift for the transition from three-dimensional (3D) Coulomb to two-dimensional (2D) interface confinement and show that the effect is experimentally observable. At B fields around 1 T, the spin-orbit Stark shift becomes as strong as that for the hyperfine interaction.

Wave-function engineering of donor spins is a basic ingredient of several quantum computing schemes^{2–4} and may also help realize novel devices based on spin degrees of freedom. In one method, an applied E field deforms the donor wave function and modifies its orbital angular momentum, which in turn can modify its spin properties through the SO interaction. This SO Stark effect is manifested by an E -field dependence of the effective g factor and can be probed by ESR experiments.⁵ However, as we are dealing with donor levels in the solid state, generally with complicated multivalley orbital-spin effects, the physical origins of this phenomenon are at present not well understood. In semiconductors with significant SO interaction, this technique can even provide a way to rotate spins by electrical modulation of the g tensor and was demonstrated in GaAs quantum dots⁸ and in

GaAs/Al_xGa_{1-x}As heterostructures.^{9,10} While the SO interaction in Si is relatively small, in a quantum computer application, such effects can lead to qubit errors at the threshold level and need to be characterized and understood, particularly, as in some proposals where the electron is controlled at the interface.^{11,12}

In this paper, we report an investigation of the Stark shift of the donor g factor in two multivalley semiconductors with varying degrees of spin-orbit interaction. We find that donors in multivalley semiconductors experience a more complicated Stark shift pattern than donors in a direct band-gap material and quantify the way in which the E field removes the isotropy of the donor g -tensor components, resulting in an anisotropic Zeeman interaction. We also compare our g -factor Stark shift for P donors in Si against measured values^{5,13} and report corresponding parameters for Ge host under different orientations of E and B fields, as a guide for future experiments. Finally, we investigate g factors of donors close to an oxide semiconductor interface and study the g -factor variation as the electron undergoes a symmetry transition from 3D Coulomb to 2D interfacial confinement.¹ This transition is central to proposals for donor-gate-confined interfacial transport and qubits in Si.^{11,12}

Engineering the magnetic field response in semiconductors typically involves compound structures, such as Al_xGa_{1-x}As or Si_xGe_{1-x}, with a spatially varying material composition. Since the two materials, Al and Ga in Al_xGa_{1-x}As, for example, have different g factors; the effective g factor of an electronic wave function can be controlled by pulling the wave function from an Al-rich part of the device to the Ga-rich part by means of an E field.³ The direct dependence of the g factor on the field in the same material, however, has been largely ignored in literature, except for Ref. 10, where the g -tensor modulation resonance was used in Al_xGa_{1-x}As heterostructures to control spin coherence electrically. In Ref. 14, an all electrical control of the spin of a Mn hole in GaAs was investigated. A large anisotropic Zeeman splitting has been reported for acceptor levels in

SiGeSi quantum wells¹⁵ and also for single-quantum states of nanoparticles.¹⁶ It was shown in Ref. 17 that the g factors of quantum-confined states are affected by atomiclike properties in addition to influences of the host material. Past ESR experiments^{13,18} have investigated the effect of uniaxial strain on donor g factors in Si and Ge, while a recent work demonstrated the gate control of spin-orbit interaction in a GaAs/AlGaAs quantum well.¹⁹

II. METHOD

We employed an atomistic tight-binding (TB) theory with a 20 orbital $sp^3d^5s^*$ basis per atom including nearest-neighbor and SO interactions. The total Hamiltonian of the host and the donor under an applied E field is

$$H = H_0 - \frac{\hbar}{4m_0^2c^2} \vec{\sigma} \cdot \vec{p} \times \vec{\nabla} V_0 + U_{\text{donor}}(r) + e\vec{E} \cdot \vec{r}. \quad (1)$$

The first term represents the host semiconductor, the second term the SO interaction of the host due to the crystal potential V_0 , and the third and the fourth represent the donor potential and the applied E field. The semiempirical TB parameters²⁰ for Si and Ge used here have been well established in literature²¹ and verified in different works.^{22,23} The SO interaction of the host was represented as a matrix element between the p orbitals of the same atom after Chadi,²⁴ and has been shown to cause energy splitting between the split-off-hole (SH) band and the degenerate manifold of the light-hole (LH) and heavy-hole (HH) bands. This representation includes both the Rashba and Dresselhaus terms inherently, as opposed to the $k \cdot p$ method, where the two are separately expressed. The donors are represented by a Coulomb potential screened by the dielectric constant of the host. The potential at the donor site U_0 was adjusted to obtain the ground-state (GS) binding energy²⁵ taking into account the valley-orbit interaction in multivalley semiconductors.²⁶ The total Hamiltonian was solved by a parallel block Lanczos algorithm to obtain the relevant donor states. A typical simulation involved about 3 million atoms and requires about 5 h on 40 processors.²⁷ The Zeeman Hamiltonian was then evaluated perturbatively, using the matrix elements $H_{Zij} = \langle \Psi_i(\vec{r}, \vec{E}) | (\vec{L} + 2\vec{S}) \cdot \vec{B} | \Psi_j(\vec{r}, \vec{E}) \rangle$, where i, j represent \uparrow and \downarrow spins of a donor state, and \vec{L} and \vec{S} denote the orbital and spin angular momentum operators, respectively. The g factor was then evaluated using the lowest spin states (ϵ), $g(\vec{E}) = (\epsilon_{\uparrow} - \epsilon_{\downarrow}) / \mu_B |\vec{B}|$, where μ_B is the Bohr magneton. Although a B field of 1 T has been used here, the results are also valid at larger B fields. The Zeeman energy shift is given by $g(E)\mu_B B$.

This TB model has been previously used to investigate the Stark shift of the hyperfine constant for a P donor in Si⁶ in good agreement with ESR measurements⁵ and momentum space methods.²⁸ It has also been successfully applied to interpret orbital Stark shift measurements on single As donors in Si FinFETS.¹

III. RESULTS AND DISCUSSIONS

The g factor for a donor GS in a multivalley semiconductor is influenced by two main factors. Within a single valley,

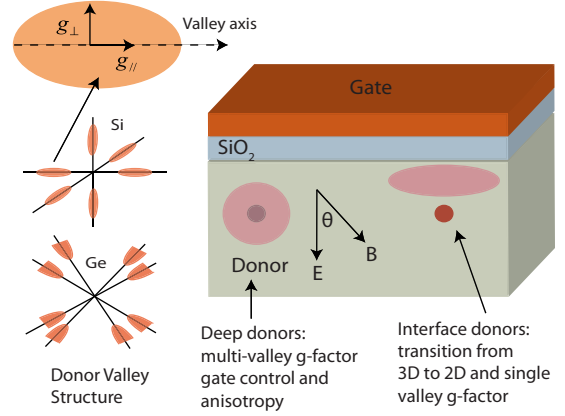


FIG. 1. (Color online) Wave function and g -factor engineering of donor and interface-confined electrons by electric and magnetic fields in Si and Ge semiconductors (CB equivalent energy surfaces shown left).

the g factors parallel (g_{\parallel}) and perpendicular (g_{\perp}) to the valley axis are different, assuming the semiconductor has non-spherical energy surfaces. This anisotropy may be affected further by external perturbations, such as strain or E fields, which can cause higher lying conduction bands (CBs) to admix with the lowest CB (Fig. 1).¹³ Second, the donor GS in Si and Ge has an equal admixture of all the valleys due to the valley-orbit interaction,²⁶ resulting in an isotropic effective g factor. Since an E field removes the equivalency of the valleys, the effective g factor becomes anisotropic depending on the contribution of the different valleys to the quantum state. The first effect was termed as the single-valley effect, while the second as the valley-repopulation effect.¹⁸ Since the full band structure is considered in the TB formalism, both effects are captured in the g factor.

Table I compares the SO properties of donors in Si and Ge, both of which are multivalley semiconductors with valleys located along [100] and [111] crystal axes, respectively. The SO interaction is stronger in Ge than in Si, as shown by the energy splitting of the SH valence band from the degenerate LH and HH light bands at the gamma point of the band structure.

Figure 2 shows that the g factor of donors primarily varies quadratically with the E field. The g -factor shifts are affected by the relative angles between the E field, the valley axis, and the B field. Figure 2(a) shows the g factor of a P donor in Si subjected to [010] E fields, while Figs. 2(b)–2(d) are for a P donor in Ge under various orientations of the E field. In Si, the [010] E field [Fig. 2(a)] removes the equivalency of the six valleys, introducing the valley-repopulation effect in the donor wave function. This results in two different parabolas for the g -factor shifts: one for $B_{\parallel}E$ and the other for $B_{\perp}E$. The [010] directed E field cannot remove the equivalency of the [111] valleys in Ge, and both parallel and perpendicular B fields produce the same g -factor shifts [Fig. 2(b)]. However, when the field is directed along the [111] valley axis as in Fig. 2(c), we obtain the split g -factor parabolas [Fig. 2(b)] similar to Fig. 2(a). In the absence of an E field, the Zeeman effect of the donor ground state is isotropic as shown by the convergence of the two parabolas at $E=0$ in both Figs. 2(a) and 2(c).

TABLE I. Comparison of the quadratic g -factor Stark shift coefficients for donors in Si and Ge under different E - and B -field orientations.

Donor (valleys) (direction)	Valence-band splitting (eV)	Binding energy (meV)	E field	B field	Theory	Expt. ^a
					$(10^{-3} \eta_2 \mu\text{m}^2/\text{V}^2)$	
Si:P (6) [100]	0.044	-45.6	[010]	B_{\parallel}	-0.012	-0.01
				B_{\perp}	0.014	(Si:Sb)
Ge:P (4) [111]	0.29	-12.8	[010]	B_{\parallel}	-4.8	
				B_{\perp}	-4.8	
			[111]	B_{\parallel}	143.8	
				B_{\perp}	-80.1	

^aReference 5.

The results of Fig. 2 are fitted to a quadratic equation $g(E)/g(0) - 1 = \eta_2 E^2$, where η_2 is the quadratic Stark coefficient. Values of η_2 are shown in Table I for a few different E - and B -field orientations. η_2 for a bulk Si:P is on the order of $10^{-5} \mu\text{m}^2/\text{V}^2$. Order-of-magnitude comparison of η_2 for Si and Ge shows that the SO Stark effect is stronger in Ge than in Si. The Zeeman anisotropy is also stronger for donors in Ge, where η_2 can differ by an order of magnitude between $B_{\parallel}E$ and $B_{\perp}E$ (Table I). The direction of the E field relative to the valley axes also affects the strength of the Zeeman interaction. This is shown by comparing the $B_{\parallel}E$ results of Ge:P for [010] and [111] directed E fields. η_2 in this case differs by almost two orders of magnitude.

Our results show good agreement in magnitude of η_2 for Si:P with the measured value for Si:Sb reported in Ref. 5 (Table I). The sign of the g -factor shift reverses between $B_{\parallel}E$ and $B_{\perp}E$ orientations if the E field is parallel to the crystal

axis. There is not sufficient experimental data to corroborate this sign reversal at present. The experiment⁵ is expected to have measured only the $B_{\perp}E$, for which a $-$ sign was reported for η_2 compared to the $+$ sign obtained here for the same orientation. We are currently unable to account for this sign discrepancy. Within the TB framework, g -factor Stark shift calculations for the single-valley GaAs case were also carried out with qualitative agreement in magnitude with the recent $k \cdot p$ work.⁷

A simple multivalley picture provides some intuitive explanations of the Stark shifted g factor based on the valley-repopulation effect. If $|a_x|^2$ represents the contribution of the $+x$ valley in Si to the donor GS, and g'_{+x} as the diagonal g tensor corresponding to this valley with the x component given by g_{\parallel} while the y and z components given by g_{\perp} , then the effective g tensor of the donor GS is given by $g(E) = \sum_{i=\pm x, \pm y, \pm z} |a_i|^2 g'_i$. Assuming $a_i = a_{-i}$ and $a_x = a_z$ for a [010] E field, we obtain the effective g -tensor components g_x , g_y , and g_z as

$$g_x = g_z = 2(|a_y|^2 + |a_x|^2)g_{\perp} + 2|a_x|^2g_{\parallel}, \quad (2)$$

$$g_y = 4|a_x|^2g_{\perp} + |a_y|^2g_{\parallel}. \quad (3)$$

These equations show that the parallel component of the g factor has a different response to the electric field as compared to the perpendicular component, verifying the split g -factor curves of Figs. 2(a) and 2(d). At $E=0$, each $a_i = 1/\sqrt{6}$, and Eqs. (2) and (3) reduce to $g_x = g_y = g_z = \frac{2}{3}g_{\perp} + \frac{1}{3}g_{\parallel} = g_0$, showing an isotropic effective g factor. At ionizing E fields, only the valleys parallel to the field contribute to the state. Setting $a_y = 1/\sqrt{2}$ and $a_x = a_z = 0$ in Eqs. (2) and (3), $g_x = g_{\perp}$ and $g_y = g_{\parallel}$, which helps to probe the single-valley g factors, as shown later in Fig. 4. For a more quantitative approach, however, one needs to know also the g -factor variation within a single valley, the precise nature of the wave-function distortion by the E field and the effect of B fields. The TB approach provides a generalized framework to include all these.

In Fig. 3, we vary the angle θ between the E and B fields from 0° to 90° for (a) Si:P under [010] E field and (b) Ge:P under [111] E field. The relative change in g factor shows a

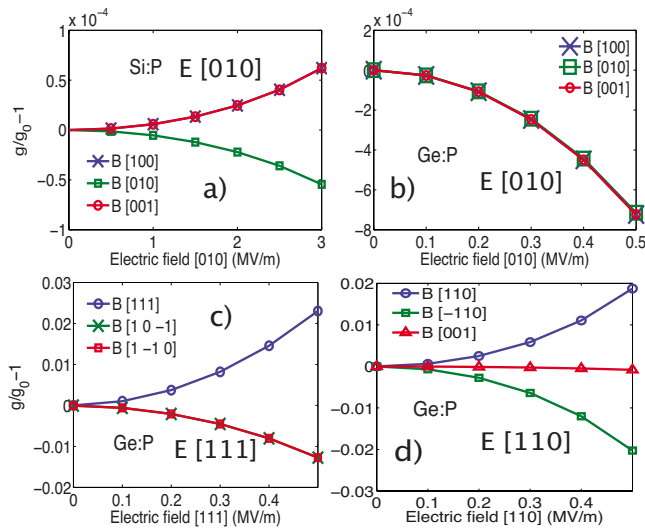


FIG. 2. (Color online) Relative change in the donor g factor in Si and Ge as a function of E -field strength (in applied direction) and for $B_{\parallel}E$ and $B_{\perp}E$. (a) Si:P with E [010], (b) Ge:P with E [010], (c) Ge:P under E [111], and (d) Ge:P under E [110]. The g -factor shift is sensitive to the relative orientation of the E and B fields with respect to the valley axis.

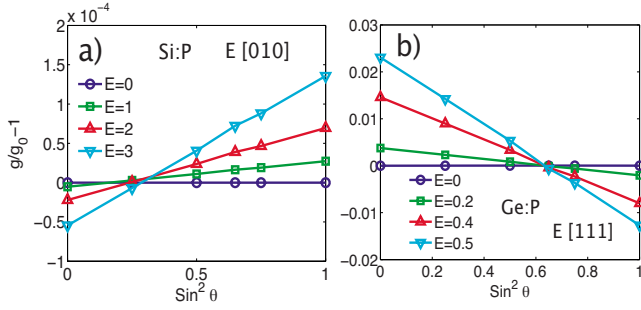


FIG. 3. (Color online) Anisotropic Zeeman effect with E field. θ represents the angle between the E field and the 1 T B field. (a) Si:P under [010] E field with B field varying from [010] to [001]. (b) Ge:P under [111] E field, with B field varying from [111] to [1-10].

linear dependence on $\sin^2 \theta$, consistent with Ref. 13. The sensitivity of this variation increases at higher E fields as shown in Figs. 3(a) and 3(b). The flat $E=0$ line indicates that the Zeeman effect is isotropic at zero field. This linear dependence of $g(E)$ on $\sin^2 \theta$ can be shown by expanding $g = [g_{\parallel}(E)^2 \cos^2 \theta + g_{\perp}(E)^2 \sin^2 \theta]^{1/2}$ up to linear terms in $\sin^2 \theta$.¹³

The confinement transition from 3D Coulomb to an interface 2D system has recently been observed (in conjunction with the theoretical approach used here)¹ and is related to a new control scheme based on dopants close to the Si-SiO₂ interface.¹¹ The donor electron can be adiabatically pulled to the interface by gate voltages^{28–30} and controlled by surface gates. We computed the g factor of a system undergoing this confinement transition. Figure 4 shows the components of the g factor parallel [Fig. 4(a)] perpendicular [Fig. 4(b)] to the E field for various donor depths. As the E field increases, the two Si conduction-band valleys in the direction of the field are lowered in energy relative to the four valleys perpendicular to the field axis. The interface state realized at ionizing E fields has contribution from these two uniaxial valleys and, hence, their g_{\parallel} and g_{\perp} approach those of the two valleys. Our simulations indicate $g_{\parallel} - g_{\perp} \approx 8 \times 10^{-3}$, which compares well on the order of magnitude with the measurements of Ref. 13. Similar g -factor anisotropies have been reported in two-dimensional electron gases.³¹ The transition to the single-valley g factors is abrupt if the donor is far away from the interface (>10 nm) and gradual if the donors are closer to the interface.^{28–30} Proximity to interfaces is also marked by linear Stark effect since the wave function becomes asymmetric due to sharp truncation by the surface. Figure 4 shows at small donor depths, the g_{\parallel} and g_{\perp} also exhibit a linear field dependence, which can even exceed the quadratic effect. A similar effect was obtained for the HF Stark effect.⁶

In a Si:P spin qubit, the ESR frequency shift of the donor electron depends both on the SO and the HF effects, as de-

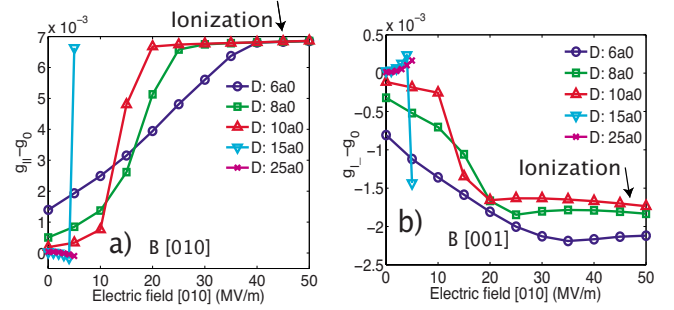


FIG. 4. (Color online) Interface effects on the donor g factor for Si:P at high E fields. g component (a) parallel, (b) perpendicular to the field, and the interface at various donor depths.

scribed by spin Hamiltonian in a z -directed B field, $\Delta H_z = \Delta g(E) \mu_B B_z S_z + \Delta A(E) I_z S_z$, where S_z and I_z are the z projections of the electronic and the nuclear spins and $A(E)$ denotes the hyperfine constant. Using the quadratic field dependencies for a bulk donor, $\Delta g(E) = -10^{-5} E^2 g(0)$ and $\Delta A(E) = -3.7 \times 10^{-3} E^2 A(0)$,⁵ we can estimate the B field at which the Zeeman shift due to SO effects becomes comparable to the hyperfine shift. With $I_z = +1/2$, $g(0) = 1.998$, $A(0) = 117.53$ MHz for Si:P and 186.8 MHz for Si:Sb,³² the B fields are 0.78 T and 1.23 T for Si:P and Si:Sb, respectively, which are within feasible operating regimes. The SO Stark effect also becomes more important than the HF effect as the electron is pulled further away from the nucleus and will dominate in the interfacial regime, where the electronic probability density at the donor site is minimal.

IV. CONCLUSION

We have applied atomistic techniques to understand and predict the E -field response of donor g factors in multivalley (Si, Ge) semiconductors with different degrees of spin-orbit interaction. The E field induces a Zeeman anisotropy that varies with the relative angle between the E and the B fields. The strength of the Stark shift is also dependent on the direction of the E field relative to the valley axis. The computed Stark shift coefficient of Si:P compares well in magnitude with limited experimental data for donors in Si. The donor g -factor Stark shift was also computed for the 3D to 2D confinement transition, suggesting that the effect is accessible to experiments.

ACKNOWLEDGMENTS

This work was supported by the Australian Research Council, NSA, and ARO (Contract No. W911NF-08-1-052). Part of the development of NEMO-3D was performed at JPL, Caltech under a contract with NASA. NCN/nanohub.org computer resources were used.

*rrahman@purdue.edu

†lloydch@unimelb.edu.au

- ¹G. P. Lansbergen, R. Rahman, C. J. Wellard, I. Woo, J. Caro, N. Collaert, S. Biesemans, G. Klimeck, L. C. L. Hollenberg, and S. Rogge, *Nat. Phys.* **4**, 656 (2008).
- ²B. E. Kane, *Nature (London)* **393**, 133 (1998).
- ³R. Vrijen, Eli Yablonovitch, K. Wang, H. W. Jiang, A. Balandin, V. Roychowdhury, T. Mor, and D. Divincenzo, *Phys. Rev. A* **62**, 012306 (2000).
- ⁴L. C. L. Hollenberg, A. S. Dzurak, C. Wellard, A. R. Hamilton, D. J. Reilly, G. J. Milburn, and R. G. Clark, *Phys. Rev. B* **69**, 113301 (2004).
- ⁵F. R. Bradbury, A. M. Tyryshkin, G. Sabouret, J. Bokor, T. Schenkel, and S. A. Lyon, *Phys. Rev. Lett.* **97**, 176404 (2006).
- ⁶R. Rahman, C. J. Wellard, F. R. Bradbury, M. Prada, J. H. Cole, G. Klimeck, and L. C. L. Hollenberg, *Phys. Rev. Lett.* **99**, 036403 (2007).
- ⁷A. De, Craig E. Pryor, and Michael E. Flatté, *Phys. Rev. Lett.* **102**, 017603 (2009).
- ⁸K. C. Nowack, F. H. L. Koppens, Yu. V. Nazarov, and L. M. K. Vandersypen, *Science* **318**, 1430 (2007).
- ⁹Y. Kato, R. C. Myers, D. C. Driscoll, A. C. Gossard, J. Levy, and D. D. Awschalom, *Science* **299**, 1201 (2003).
- ¹⁰G. Salis, Y. Kato, K. Ensslin, D. C. Driscoll, A. C. Gossard, and D. D. Awschalom, *Nature (London)* **414**, 619 (2001).
- ¹¹M. J. Calderón, B. Koiller, X. Hu, and S. Das Sarma, *Phys. Rev. Lett.* **96**, 096802 (2006).
- ¹²A. J. Skinner, M. E. Davenport, and B. E. Kane, *Phys. Rev. Lett.* **90**, 087901 (2003).
- ¹³D. K. Wilson and G. Feher, *Phys. Rev.* **124**, 1068 (1961).
- ¹⁴J.-M. Tang, J. Levy, and M. E. Flatté, *Phys. Rev. Lett.* **97**, 106803 (2006).
- ¹⁵K.-M. Haendel, R. Winkler, U. Denker, O. G. Schmidt, and R. J. Haug, *Phys. Rev. Lett.* **96**, 086403 (2006).
- ¹⁶J. R. Petta and D. C. Ralph, *Phys. Rev. Lett.* **89**, 156802 (2002).
- ¹⁷C. E. Pryor and M. E. Flatté, *Phys. Rev. Lett.* **96**, 026804 (2006).
- ¹⁸L. Roth, *Phys. Rev.* **118**, 1534 (1960).
- ¹⁹M. Studer, G. Salis, K. Ensslin, D. C. Driscoll, and A. C. Gossard, *Phys. Rev. Lett.* **103**, 027201 (2009).
- ²⁰J. C. Slater and G. F. Koster, *Phys. Rev.* **94**, 1498 (1954).
- ²¹T. B. Boykin, G. Klimeck, and F. Oyafuso, *Phys. Rev. B* **69**, 115201 (2004).
- ²²G. Klimeck, F. Oyafuso, T. B. Boykin, R. Chris Bowen, and Paul von Allmen, *Comput. Model. Eng. Sci.* **3**, 601 (2002).
- ²³G. Klimeck, S. S. Ahmed, Hansang Bae, N. Kharche, S. Clark, B. Haley, Sunhee Lee, M. Naumov, Hoon Ryu, F. Saied, M. Prada, M. Korkusinski, T. B. Boykin, and R. Rahman, *IEEE Trans. Electron Devices* **54**, 2079 (2007).
- ²⁴D. J. Chadi, *Phys. Rev. B* **16**, 790 (1977).
- ²⁵S. Ahmed, N. Kharche, R. Rahman, M. Usman, S. Lee, H. Ryu, H. Bae, S. Clark, B. Haley, M. Naumov, F. Saied, M. Korkusinski, R. Kennel, M. McLennan, T. B. Boykin, and G. Klimeck, in *Multimillion Atom Simulations with NEMO 3-D*, edited by R. A. Meyers, Springer Encyclopedia of Complexity and Systems Science (Springer-Verlag GmbH, Heidelberg, 2009), pp. 5745–5783.
- ²⁶W. Kohn and J. M. Luttinger, *Phys. Rev.* **98**, 915 (1955).
- ²⁷nanoHUB.org computational resource of a 256-node 3.3GHz Pentium Irwindale PC cluster was used. The TB simulations were done with the Nano-Electronic Modeling Tool (NEMO-3D).
- ²⁸C. J. Wellard and L. C. L. Hollenberg, *Phys. Rev. B* **72**, 085202 (2005).
- ²⁹A. S. Martins, R. B. Capaz, and Belita Koiller, *Phys. Rev. B* **69**, 085320 (2004).
- ³⁰G. D. J. Smit, S. Rogge, J. Caro, and T. M. Klapwijk, *Phys. Rev. B* **70**, 035206 (2004).
- ³¹R. Winkler, S. J. Papadakis, E. P. De Poortere, and M. Shayegan, *Phys. Rev. Lett.* **85**, 4574 (2000).
- ³²H. Overhof and U. Gerstmann, *Phys. Rev. Lett.* **92**, 087602 (2004).